

Natural convection in partitioned rectangular air enclosures

Samy M. El-Sherbiny

Mechanical Eng. Dept., Faculty of Eng., Alexandria University, Alexandria, Egypt

A numerical study is presented to investigate the effects of using different configurations of solid partitions on the natural convection in inclined air-filled rectangular enclosures. A finite-difference scheme is used to solve the governing equations for mass, momentum and energy conservation. Flow patterns of streamlines and isotherms for different cases are developed to investigate the effects of the layer and partition configurations on the flow field and heat transfer characteristics. Local and average Nusselt numbers are presented as a function of the governing parameters. The effects of the number of partitions and their location on the average Nusselt number are also investigated. The study covered a wide range of the partition parameters for aspect ratios of 0.5 and 1.0 in the Rayleigh number range $10^3 \leq Ra \leq 10^6$. The results showed a strong influence of the partition location and height on the heat transfer. Increasing the partition height and number causes an increase in the insulating effect of the partitions.

يقدم البحث دراسة عددية لتأثير استخدام حواجز صلبة بأشكال وأوضاع مختلفة داخل طبقة من الهواء مستطيلة الشكل ومائلة. أحد جوانب الطبقة ساخن والجانب المقابل له بارد أما السطحان الأخران فهما في حالة عزل حراري تام. المعادلات التفاضلية التي تحكم انتقال الكتلة وكمية الحركة والطاقة تم حلها عددياً باستخدام برنامج حاسب آلي في حالة الحمل الحر عند حالات مختلفة من أبعاد وأوضاع الحواجز وعند مدى واسع لرقم رالي بين 10^3 و 10^6 وذلك لطبقات ذات نسبة أبعاد 0.5 ، 1.0. تم عرض النتائج في منحنيات تبين خطوط السريان ودرجات الحرارة في حالات مختلفة كما تم عرض تأثير العناصر المختلفة للدراسة على كل من رقمي نوسلت الموضعي والمتوسط. وقد أظهرت الدراسة أهمية استخدام الحواجز لتقليل كمية الحرارة المفقودة بالحمل الحر داخل الطبقات الهوائية. كما بينت الدراسة أن رقم نوسلت المتوسط يقل مع زيادة طول وسمك الحاجز ويزداد مع زيادة رقم رالي. استخدام حاجز واحد في الجانب المعزول العلوي يقلل كمية الحرارة بحد أقصى 18.7% ويزداد تأثيره كلما اقترب من السطح البارد. أما استخدام حاجزين على الجانبين المعزولين فإنه يقلل الحرارة المفقودة بحد أقصى 37.5% من الحالة الخالية من الحواجز. رقم نوسلت المتوسط في الطبقة الهوائية يكون أكبر ما يمكن عند زاوية ميل 60° مع الأفقي.

Keywords: Natural convection, Enclosures, Partitioned cavity, Rectangular layers

1. Introduction

The natural convection heat transfer across an air gap is of importance in a large number of engineering situations. It is of particular importance in double-glazed windows and flat-plate solar collectors where it can constitute the main mode of heat loss. Some investigators [1-2] have tried to suppress this major heat loss using honeycomb materials inserted in the air gap to retard the critical Rayleigh number at which convection starts. Another technique for suppressing convection within the air gap is to use internal partitions. These partitions block the normal convective flow and provide additional shear surfaces to retard the motion. Partitions are used to increase the thermal resistance of fluid-filled enclosed cavities and thus reduce the convective heat transfer loss

in the enclosure. Applications include thermal insulation, design of passive solar heating systems, room ventilation and fire prediction. The insertion of baffles should be suitably placed and stretched in the cavity to get the purpose of their use.

Emery [3] inserted a vertical baffle centrally located in vertical enclosed glycerin-filled cavities of aspect ratio, $A=10$ and 50 . The baffle was not touching the end walls with a height ratio, S equals 0.9 . Therefore, it did not affect the boundary layers on the end walls and thus did not greatly disturb the basic flow within the cavity since it is in the relatively stagnant central core. The presence of such a baffle did not produce any significant change in the heat transfer across the cavity. The insertion of end baffles in the cross-flow boundary layers at the end walls (see fig. 1)

would affect the flow pattern and thus modify the convective heat transfer.

An experimental investigation of natural convection in a vertical enclosure with $A=1$ having partitions protruding into the cavity from the adiabatic end walls was presented by Bajorek and Lloyd [4]. Local and average Nusselt numbers were determined using a Mach-Zehnder interferometer for air and carbon dioxide filled enclosures in the Grashof number range $1.7 \times 10^5 \leq Gr \leq 3 \times 10^6$. The partitions were found to significantly reduce the convective heat transfer.

Mynett and Duxbury [5] and Nansteel and Greif [6] have studied the effects of a single partition which is suspended from the ceiling of a vertical enclosure. Temperature profiles were obtained and dye was injected into the enclosure to visualize the flow. Correlations were obtained giving the average Nusselt number as a function of Rayleigh number, partition conductance and a parameter describing the partition height. Janikowski et al. [7] used a Mach-Zehnder interferometer to investigate natural convection in an air-filled, two-dimensional enclosure with solid and porous partitions protruding from both the floor and ceiling of the enclosure into the cavity. Local and average heat transfer coefficients were obtained for an enclosure with aspect ratio of 5 at a Grashof number of 1.1×10^6 . A numerical study of the laminar natural convection for water inside a vertical partially-divided cavity was presented by Winters [8]. The partial divider was centrally located at the top or the bottom end walls. Two contrasting cases of an insulated and a conducting partition were considered. The study was performed for aspect ratio, $A =$ partition location ratio, $R =$ partition height ratio, $S = 0.5$ and a thickness ratio, $C = 0.062$ (see fig. 1) in the range $10^7 \leq Ra \leq 5 \times 10^9$. The calculated average Nusselt number was in good agreement with the experimental data presented by Nansteel and Greif [6] for aluminum partition in water.

Nansteel and Greif [9] performed experiments in vertical layers filled with high Prandtl number silicon oils ($620 \leq Pr \leq 910$) in the range $1.6 \times 10^9 \leq Ra \leq 5.9 \times 10^9$. Ceiling-mounted vertical partitions of low thermal conductivity and various lengths were used at

$R=0.5$ and for $A=0.5$. Correlations were obtained giving the dependence of Nusselt number on Rayleigh number and partition length.

The effects of using a horizontal partition attached to the center of the cold surface in a vertical rectangular air layer were numerically investigated by Oosthuizen and Paul [10]. Aspect ratios between 3 and 7 were tested for $8 \times 10^2 \leq Ra \leq 8 \times 10^3$ and various plate heights. The results indicated that the partition has increased the local Nusselt number on the upper portion of the hot wall and decreased it near the center. However, the average Nusselt number was slightly increased.

Tsang and Acharya [11] investigated numerically the effects of an off-center complete partition parallel to the isothermal surfaces in an inclined air cavity with $A=1$. The study covered the ranges $10^4 \leq Ra \leq 10^7$ and $30^\circ \leq \varphi \leq 90^\circ$ for partition locations of $R=0.75$ and 0.875 . The results indicated a significant influence of the partition location on the flow and heat transfer characteristics. The average Nusselt number over the hot surface was found to be significantly smaller than the corresponding value for a non-partitioned enclosure.

A numerical study for laminar and turbulent natural convection in vertical enclosures with partial partitions has been performed by Bilgen [12]. The study covered aspect ratios, A from 0.3 to 0.4, partition location ratios, R from 0.5 to 0.6, height ratios, S from 0 to 0.15 and Rayleigh numbers in the range $10^4 \leq Ra \leq 10^{11}$. Isotherms and streamlines were produced for various Ra and geometrical conditions and correlations were given. Also, an experimental study in an air-filled vertical partitioned square cavity was performed by Ampofo [13] for $Ra=1.58 \times 10^9$ where velocities and temperatures were measured and local and average Nusselt numbers were presented.

Khalifa et al. [14-16] conducted a series of experiments on the effects of 14 different configurations of adiabatic partitions in vertical layers with $A=0.5$. This includes partitions with a central or lateral opening. The study covered the ranges $6 \times 10^7 \leq Ra \leq 1.5 \times 10^8$ in air and $10^{11} \leq Ra \leq 7 \times 10^{11}$ in water. Correlations were given and the

percentage reduction in heat transfer is reported for each case compared to the case of undivided layer. The effects of inclination angle and the number of partitions on flow fields and Nusselt number were numerically investigated by Said et al [17] for the natural turbulent flow in the rectangular layer.

2. Mathematical analysis

A sketch of the two-dimensional rectangular partitioned layer is shown in fig. 1. It consists of two inclined parallel isothermal surfaces at different temperatures, T_h and T_c while the other two surfaces are adiabatic. Solid partitions of thickness, t and height, d are fixed to the adiabatic walls, as shown in fig. 1, at a distance, w from either of the isothermal surfaces. The layer is filled with air ($Pr = 0.71$) which is considered Newtonian with constant properties except for the density in the buoyancy force. The Boussinesq approximation is used to relate the variable density to the local temperature.

2.1. Governing equations

The dimensionless steady-state equations for mass, momentum and energy in the Cartesian coordinates (X, Y) are given as follows:

$$\frac{\partial U}{\partial X} + \frac{\partial V}{\partial Y} = 0, \quad (1)$$

$$U \frac{\partial U}{\partial X} + V \frac{\partial U}{\partial Y} = -\frac{\partial P_d}{\partial X} + Pr \left(\frac{\partial^2 U}{\partial X^2} + \frac{\partial^2 U}{\partial Y^2} \right) + \quad (2)$$

$$Ra \cdot Pr \cdot (\theta - 1) \sin \phi,$$

$$U \frac{\partial V}{\partial X} + V \frac{\partial V}{\partial Y} = -\frac{\partial P_d}{\partial Y} + Pr \left(\frac{\partial^2 V}{\partial X^2} + \frac{\partial^2 V}{\partial Y^2} \right) + \quad (3)$$

$$Ra \cdot Pr \cdot (\theta - 1) \cos \phi,$$

$$U \frac{\partial \theta}{\partial X} + V \frac{\partial \theta}{\partial Y} = \frac{\partial^2 \theta}{\partial X^2} + \frac{\partial^2 \theta}{\partial Y^2}. \quad (4)$$

Where,

$$U = \frac{u}{\alpha / L}, \quad V = \frac{v}{\alpha / L}, \quad X = x / L, \quad Y = y / L,$$

$$P_d = \frac{P_d}{\rho \alpha^2 / L^2}, \quad \theta = \frac{T - T_c}{T_h - T_c},$$

$$Ra = \frac{\beta g (T_h - T_c) L^3}{\nu \alpha}, \quad Pr = C_p \mu / k, \quad \text{and}$$

$$Gr = \frac{\beta g (T_h - T_c) L^3}{\nu^2}$$

The layer and partition configurations are defined by the following dimensionless parameters:

Aspect ratio, $A = H/L$; Location ratio, $R = w/L$; Height ratio, $S = d/H$ and Thickness ratio, $C = t/L$.

2.2. Boundary conditions

The boundary conditions on the surfaces of the air enclosure are given as follows:

$$\text{at } Y = 0, 0 \leq X \leq A: U = 0, V = 0, \theta = 1;$$

$$\text{at } Y = 1, 0 \leq X \leq A: U = 0, V = 0, \theta = 0;$$

$$\text{at } X = 0, 0 \leq Y \leq 1: U = 0, V = 0, \frac{\partial \theta}{\partial X} = 0; \text{ and}$$

$$\text{at } X = A, 0 \leq Y \leq 1: U = 0, V = 0, \frac{\partial \theta}{\partial X} = 0$$

Inside the solid partition, the conduction equation is solved and continuity of heat flux across the solid/fluid interface is ensured. Thus, the boundary conditions for the partitions are given as:

a) For upper partition

$$\text{at } A(1-S) \leq X \leq A, Y = R \pm 0.5 C: U=0, V=0, \left(\frac{\partial \theta}{\partial Y} \right)_f = \frac{k_s}{k} \left(\frac{\partial \theta}{\partial Y} \right)_s, \text{ and}$$

$$\text{at } X = A(1-S), R-0.5 C \leq Y \leq R+0.5 C: U=0, V=0, \left(\frac{\partial \theta}{\partial X} \right)_f = \frac{k_s}{k} \left(\frac{\partial \theta}{\partial X} \right)_s$$

b) For lower partition,

at $0 \leq X \leq S$, $Y = 1-R \pm 0.5 C$: $U=0$, $V=0$,
 $\left(\frac{\partial\theta}{\partial Y}\right)_f = \frac{k_s}{k} \left(\frac{\partial\theta}{\partial Y}\right)_s$, and

at $X = S$, $1-R - 0.5 C \leq Y \leq 1-R + 0.5 C$: $U=0$,
 $V=0$, $\left(\frac{\partial\theta}{\partial X}\right)_f = \frac{k_s}{k} \left(\frac{\partial\theta}{\partial X}\right)_s$.

Where, the subscripts, (f) and (s) refer to fluid and solid sides of the solid/fluid interface respectively. The value of k_s/k is taken as 10^4 for a highly conducting partition material in an air enclosure.

2.3. The Nusselt number

The local Nusselt number at any point on the hot surface, Nu_x is defined as:

$$Nu_x = \frac{h_x L}{k} = -\left(\frac{\partial\theta}{\partial Y}\right)_{Y=0}, \quad (5)$$

and the average Nusselt number over the hot surface, Nu is calculated as:

$$Nu = \frac{hL}{k} = -\frac{1}{A} \int_0^A \left(\frac{\partial\theta}{\partial Y}\right)_{Y=0} dX. \quad (6)$$

3. Numerical solution

The above governing equations along with their boundary conditions are solved using the SIMPLER algorithm developed by Patankar [18]. These equations were first expressed in a finite difference form using central differences in space. Then, the discretized equations were solved by Gauss-Seidel elimination method. A line by line procedure of iteration is used which is a combination of the direct method and the resulting Tri-Diagonal Matrix Algorithm (TDMA). The under-relaxation successive iteration method is used starting from stagnant initial conditions until steady-state conditions were reached. The Nusselt number is then calculated using the converged solution of the temperature field. The iteration is stopped when the variation in the average Nusselt number over 100 iterations is less

than 0.01% of its value. Less than 1500 iterations were enough for most of the cases to reach the required accuracy. Higher Rayleigh numbers and low angles of inclination required higher number of iterations. A grid independence study is conducted using three different uniform grids with 22×22 , 32×32 and 42×42 nodes. It was shown that a further reduction in mesh size does not have any significant effect on the average Nusselt number. Therefore, for all calculations, the enclosure was divided into a 42×42 grid to obtain the present results. According to the numerical technique proposed by Patankar [18], only the first and last control volumes in each coordinate have zero thickness and the rest (40 control volumes) are uniform with equal thickness.

4. Results

In the present study, two different partition configurations are investigated. The first is a layer with only one single top partition at $X = A$, and the second with two asymmetric partitions as shown in fig. 1. The study covers the ranges $10^3 \leq Ra \leq 10^6$, $30^\circ \leq \varphi \leq 180^\circ$, $0 \leq S \leq 0.75$, $0 \leq R \leq 0.75$, $0.05 \leq C \leq 0.10$ for $A = 0.5$ and 1.0 .

4.1. Single top partition

The streamlines and isotherms for a vertical square cavity with a single partition at the center of the top adiabatic surface are shown in fig. 2 with $S = 0.25$ and $C = 0.10$. For $Ra = 10^3$, the unicellular flow is produced with its center lowered due to the presence of the partition. The isotherms are slightly deviated from being parallel since the flow is still in the conduction regime. For $Ra = 10^6$, the flow field is stronger and fills the whole cavity with a shift towards the cold surface. The isotherms indicate the laminar boundary layer regime with a higher heat flux at the bottom of the hot surface and the top of the cold one. A vertical temperature gradient is shown in the core of the cavity.

The effects of partition height and thickness as well as the Rayleigh number are shown in fig. 3. In general, the average Nusselt number increases with the increase in Ra . The

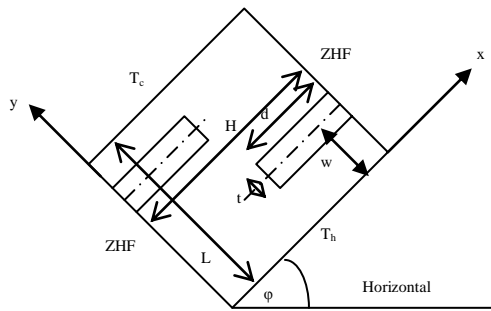


Fig. 1. The partitioned layer.

case of no partitions gives the highest heat transfer. Increasing the partition height causes a continuous decrease in Nusselt number with a higher influence at higher Ra . Increasing the partition thickness ratio from 0.05 to 0.10 causes a slight decrease in Nu which is more pronounced at higher values of S and Ra .

The effect of partition location ratio, R on the average Nusselt number is given in fig. 4. The partition location was changed from near

the hot to near the cold surfaces. Placing the partition close to the cold surface at $R = 0.75$ has the highest reduction in heat transfer across the cavity for $Ra \geq 2 \times 10^4$. At $Ra = 10^6$, the effect of the partition location is almost negligible.

For a shallow vertical air layer with $A=R=S=0.5$ and $C=0.1$, the effects of the top partition on streamlines and isotherms are shown in fig. 5. For $Ra=10^3$, the partition divided the flow into two big unicellular cells with weak flow between the two compartments. The isotherms are almost parallel vertical lines indicating pure conduction regime. For $Ra=10^6$, the flow is stronger with higher flow rates between the two sides of the partition and stronger field close to the cold surface. The isotherms indicate the fully developed laminar boundary layer regime with high temperature gradients near the bottom of the hot surface and the top of the cold one.

The heat transfer data for $A=0.5$ are shown in fig. 6. Increasing the partition height ratio,

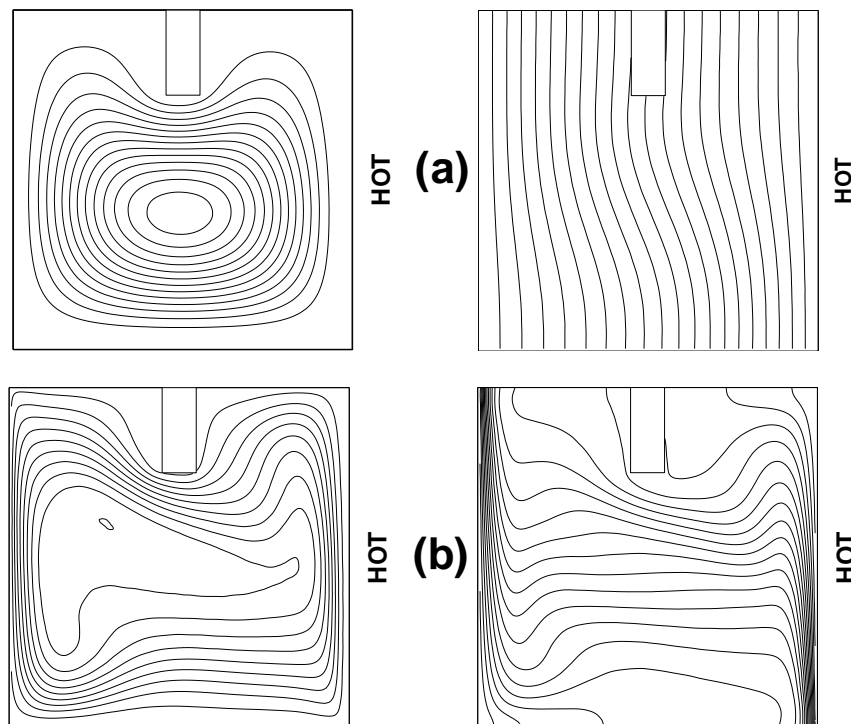


Fig. 2. Streamlines (left) and isotherms (right) ($A=1, \varphi=90^\circ, R=0.5, S=0.25$ and $C=0.1$) (a) $Ra=10^3$, (b) $Ra=10^6$.

S increases the insulating effect with higher reduction in the average Nusselt number at higher Rayleigh numbers. Comparing the results in figs. 3 and 6, we find that decreasing the aspect ratio from $A=1$ to $A=0.5$ results in a significant decrease in the average Nusselt numbers. The effects of partition on local Nusselt numbers are shown in fig. 7 for a vertical square cavity with a central top partition with $C=0.10$. For $Ra=10^4$, the partition causes a high reduction (30 %) in Nu_x near the bottom of the hot surface. This value increases to 56 % at the middle of the

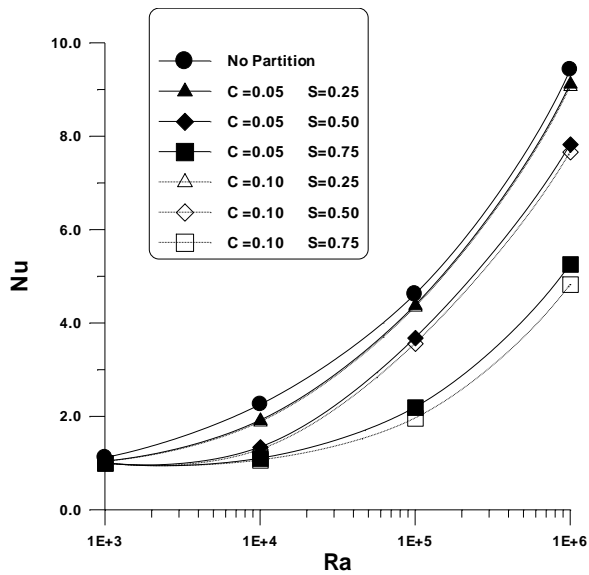


Fig. 3. Effects of partition height, thick and Ra on Nu ($A = 1$, $\varphi = 90^\circ$ and $R = 0.5$).

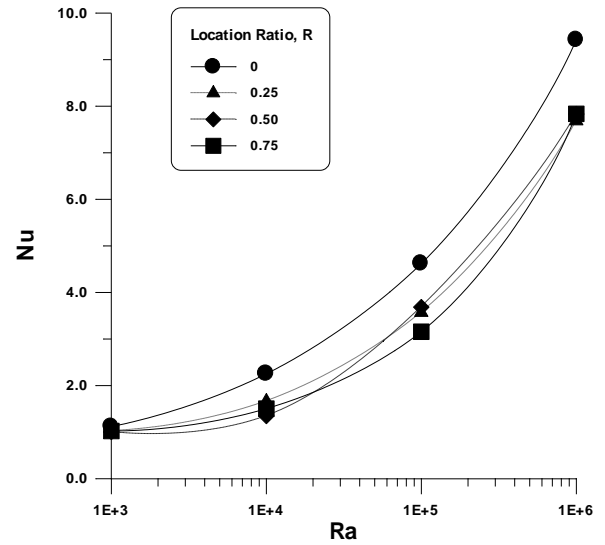


Fig. 4. Effect of partition location on Nu ($A = 1$, $\varphi = 90^\circ$, $S = 0.5$ and $C = 0.05$).

hot surface, and then it continuously decreases to zero at the top of the hot plate. For $Ra=10^6$, a very small drop in Nu_x (1.3 %) occurs near the bottom of the hot surface due to the presence of the used partition. This value gradually increases to 75% at the top of the hot surface.

The effect of inclination angle, φ on the average Nusselt number is shown in fig. 8 for a square cavity with a central top partition with $S=0.5$ and $C=0.1$. For $Ra = 10^5$ and 10^6 , a

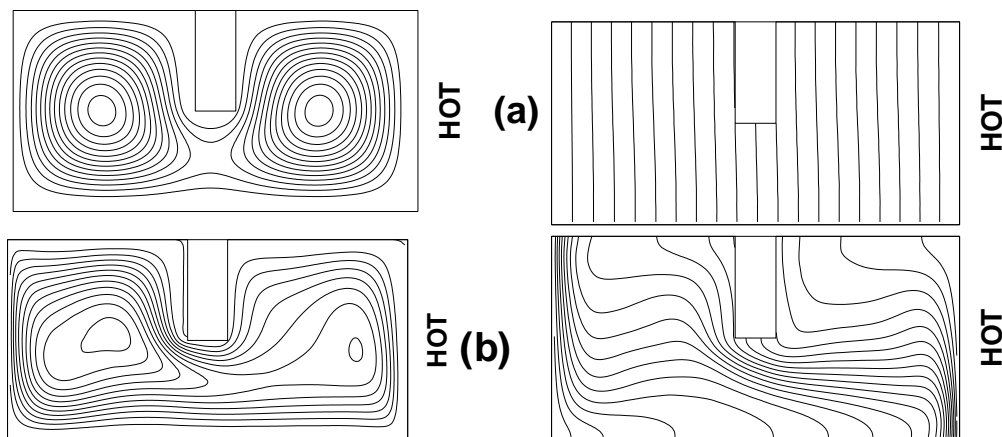


Fig. 5. Streamlines (left) and isotherms (right) ($A=0.5$, $\varphi=90^\circ$, $R=0.5$, $S=0.50$ and $C=0.1$) (a) $Ra=10^3$, (b) $Ra=10^6$.

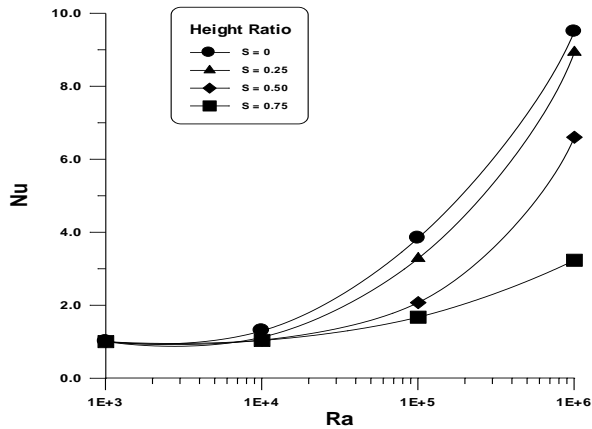


Fig. 6. Effects of partition height and Ra on Nu ($A = 0.5$, $\varphi = 90^\circ$, $R = 0.5$ and $C = 0.10$).

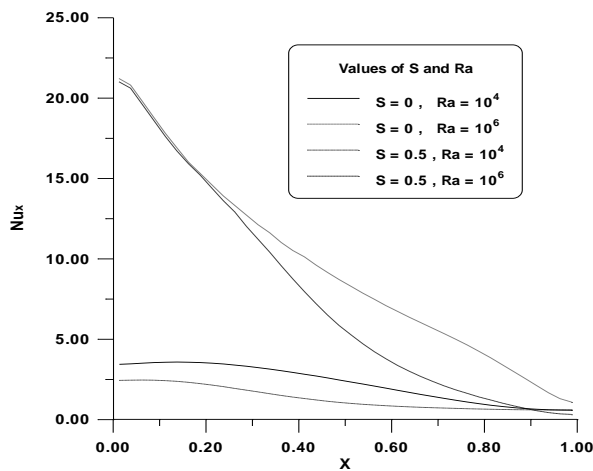


Fig. 7. Effects of partition on local Nusselt number ($A = 1$, $\varphi = 90^\circ$, $R = 0.5$ and $C = 0.1$).

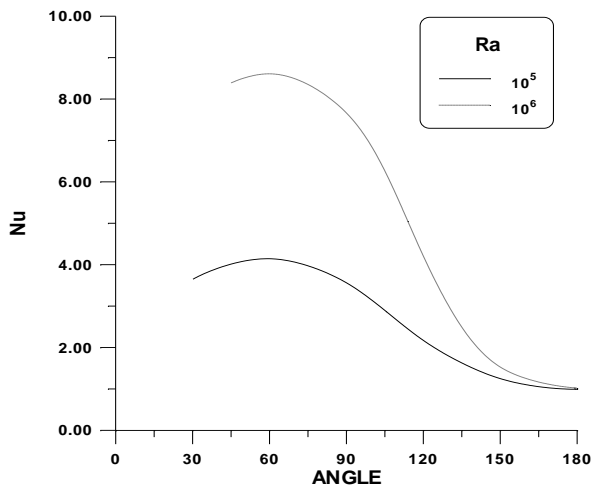


Fig. 8. Effect of inclination angle ($A = 1$, $R = 0.5$, $S = 0.5$ and $C = 0.1$).

maximum value of Nu occurs at $\varphi = 60^\circ$. This value gradually decreases to $Nu=1$ (pure conduction) at $\varphi = 180^\circ$.

4.2. Two partitions

In this case, the vertical square air layer is fitted with two partitions of $S=0.25$ and $C=0.1$; one on the top adiabatic side wall and the other on the bottom one. These partitions are either identically offset towards the hot and cold surfaces, as shown in fig. 9-a, with $R=0.25$ or are positioned centrally ($R=0.5$) as in fig. 9-b. The streamlines and isotherms for $Ra=10^5$ are shown in fig. 9-a for $R=0.25$. A distorted unicellular flow is produced with its center of rotation at the cavity center. The isotherms indicate the boundary layer type of flow. When the partitions are moved to the center ($R=0.5$), fig. 9-b shows the streamlines compressed between the two partitions with complete separation in the center of the cells. The isotherms represent the boundary layer flow with lower local Nusselt numbers at the top of the hot plate for $R=0.50$ than that for $R=0.25$.

The effects of the number of partitions and their location on Nu are shown in fig. 10. The layer with no partitions always gives the higher value of Nu . Using a single top partition decreases Nu by about 18.7 % at $Ra=10^4$. This value decreases to 6 % at $Ra=10^6$. On the other hand, using two partitions decreases Nu by about 37.5 % at $Ra=10^4$. Again, this value decreases to 12.7 % at $Ra=10^6$. In general, increasing the number of partitions increases the insulating effect of the air layer.

5. Conclusions

The effects of using partitions of different configurations in an inclined air rectangular enclosure are numerically investigated. The study covered a wide range of the parameters affecting the flow and heat transfer. Streamlines and isotherms are generated to explain the flow regimes. Local and average Nusselt numbers are presented for different cases. The study shows that the average Nusselt number decreases with the increase of partition height and thickness and increases

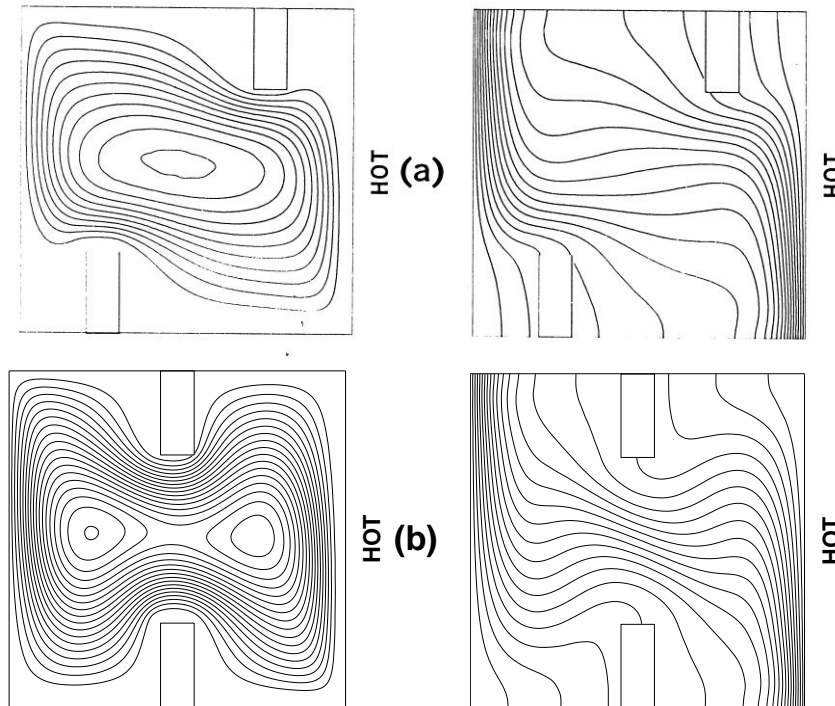


Fig. 9. Streamlines (left) and isotherms (right) ($A = 1$, $\varphi=90^\circ$, $Ra = 10^5$, $S = 0.25$ and $C=0.1$) (a) $R=0.25$, (b) $R=0.50$.

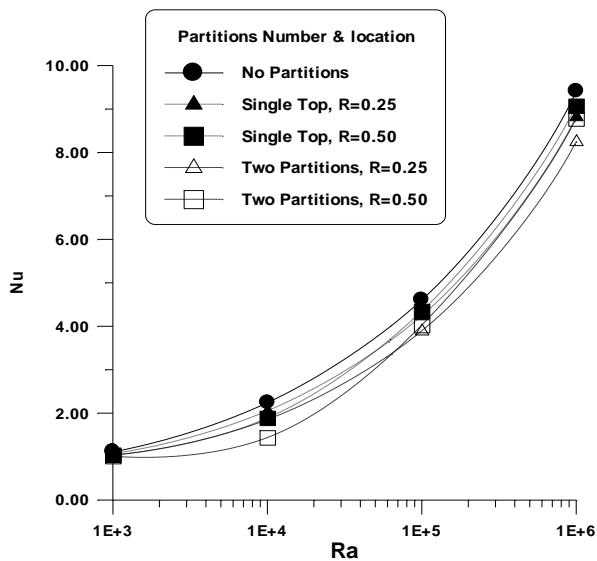


Fig. 10. Effects of number of partitions and locations on Nu ($A = 1$, $\varphi = 90^\circ$, $S = 0.25$ and $C = 0.1$).

with the increase in Ra . Locating the top partition closer to the cold surface increases the insulating effect of the air layer. The maximum heat transfer in partitioned square air layers occurs in layers inclined at $\varphi = 60^\circ$.

Using a single top partition decreases the average Nusselt number by a maximum of 18.7 % while using two asymmetric partitions decreases Nu by a maximum of 37.5 % relative to the simple non-partitioned layer.

Nomenclature

- A is the cavity aspect ratio, H/L ,
- C is the thickness ratio, t/L ,
- C_p is the specific heat at constant pressure, $J/kg.K$,
- d is the partition height, m ,
- g is the gravitational acceleration, m/s^2 ,
- Gr is the Grashof number, $\beta g (T_h - T_c) L^3 / \nu^2$,
- H is the average heat transfer coefficient, $W/m^2 K$,
- h_x is the local heat transfer coefficient, $W/m^2 K$,
- H is the cavity height, m ,
- k is the fluid thermal conductivity, $W/m.K$,
- k_s is the partition thermal conductivity, $W/m.K$,

L is the cavity width (plate spacing), m,
 Nu is the average Nusselt number, hL/k ,
 Nu_x is the local Nusselt number, $h_x L/k$,
 p_d is the dynamic pressure, N/m²,
 P_d is the dimensionless dynamic pressure,
 Pr is the Prandtl number, $C_p \mu/k$,
 R is the location ratio, w/L ,
 Ra is the Rayleigh number, $\beta g(T_h - T_c) L^3/av$,
 S is the Height ratio, d/H ,
 t is the partition thickness, m,
 T is the temperature, K,
 T_c is the temperature of cold surface, K,
 T_h is the temperature of hot surface, K,
 u is the velocity in x-direction, m/s,
 U is the dimensionless velocity in x-direction,
 v is the velocity in y-direction, m/s,
 V is the dimensionless velocity in y-direction,
 W is the partition location, m,
 x, y is the Cartesian coordinates, and
 X, Y is the dimensionless coordinates.

Greek

a is the thermal diffusivity, m²/s,
 β is the volumetric coefficient of thermal expansion, 1/K,
 θ is the dimensionless temperature,
 μ is the dynamic viscosity, kg/m.s,
 ν is the kinematic viscosity, m²/s,
 ρ is the density, kg/m³, and
 ϕ is the angle of tilt from horizontal, rad.

References

- [1] W.W.S Charters and L.F Peterson, "Free Convection Suppression Using Honeycomb Cellular Materials", *Solar Energy*, Vol. 13, pp. 353-360 (1972).
- [2] K.G.T. Hollands, "Natural Convection in Horizontal Thin-Walled Honeycomb Panels", *J. Heat Transfer*, Vol. 95, pp. 439-443 (1973).
- [3] A.F. Emery, "Exploratory Studies of Free Convection Heat Transfer Through an Enclosed Vertical Liquid Layer With A Vertical Baffle", *J. Heat Transfer*, Vol. 91, pp. 163-164 (1969).
- [4] S.M. Bajorek and J.R. Lloyd, "Experimental Investigation of Natural Convection in Partitioned Enclosures", *J. Heat Transfer*, Vol. 104, pp. 527-532 (1982).
- [5] J.A. Mynett and D. Duxbury, "Temperature Distributions Within Enclosed Plane Air Cells Associated With Heat Transfer by Natural Convection", *Proc. of the 5th Int. Heat Transfer Conf.*, Vol. 3, pp. 13-31 (1974).
- [6] M.W. Nansteel and R. Greif, "Natural Convection in Undivided and Partially Divided Rectangular Enclosures", *J. Heat Transfer*, Vol. 103, pp. 623-629 (1981).
- [7] H.E. Janikowski, J. Ward and S.D. Probert, "Free Convection in Vertical Air-Filled Rectangular Enclosures Fitted With baffles", *Proc. of the 6th Int. Heat Transfer Conf.*, Vol. 6, pp. 257-263 (1978).
- [8] K.H. Winters, "Laminar Natural Convection in a Partially-Divided Cavity", *Proc. of the 3rd Int. conf. on Numerical Methods in Thermal Problems*, Seattle, USA, pp. 563-573 (1983).
- [9] M.W. Nansteel and R. Greif, "Natural Convection Heat Transfer In Complex Enclosures at Large Prandtl Number", *J. Heat transfer*, Vol. 105, pp. 912-915 (1983).
- [10] P.H. Oosthuizen and J.T. Paul, "Free Convective Heat Transfer in Cavity Fitted With a Horizontal Plate on the Cold Wall", *Proc. of the 23rd. National Heat Transfer Conf.*, Denver, Colorado, HTD-Vol. 43, pp. 101-107 (1985).
- [11] C.H. Tsang and S. Acharya, "Natural Convection in an Inclined Enclosure With an Off- Center Complete Partition", *Num. Heat Transfer*, Vol. 9, pp. 217-239 (1986).
- [12] E. Bilgen, "Natural Convection in Enclosures With Partial Partitions", *Renewable Energy*, Vol. 26 (2), pp. 257-270 (2002).
- [13] F. Ampofo, "Turbulent Natural Convection in air Filled Partitioned Square", *Int. Jour. of Heat and Fluid Flow*, Vol. 25 (1), pp. 103-114 (2004).

- [14] A.J.N. Khalifa and S.E. Abdullah, "Buoyancy Driven Convection in Undivided and Partially Divided enclosures", *Energy Conversion and Management*, Vol. 40 (7), pp. 717-727 (1999).
- [15] A.J.N. Khalifa and W.K. Sahib, "Turbulent Buoyancy Driven Convection in Partially Divided Enclosures", *Energy Conversion and Management*, Vol. 43 (16), pp. 2115-2121 (2002).
- [16] A.J.N. Khalifa and A.F. Khudheyr, "Natural Convection in Partitioned Enclosures: Experimental Study on 14 Different Configurations", *Energy Conversion and Management*, Vol. 42 (6), pp. 653-661 (2001).
- [17] S.A.M. Said, M.A. Habib and M.A.R. Khan, "Turbulent Natural Convection Flow in Partitioned Enclosures", *Computers and Fluids*, Vol. 26 (6), pp. 547-563 (1997).
- [18] S.V. Patankar, "Numerical Heat Transfer and Fluid Flow", Mc Graw-Hill, New York (1980).

Received September 13, 2004
Accepted September 29, 2004